Heat Flux Determination From Measured Heating Rates Using Thermographic Phosphors

D. G. Walker
Department of Mechanical Engineering,
Vanderbilt University,
Nashville, TN 37235-1592
e-mail: greg.walker@vanderbilt.edu

A new method for measuring the heating rate (defined as the time rate of change of temperature) and estimating heat flux from the heating rate is proposed. The example problem involves analytic heat conduction in a one-dimensional slab, where the measurement location of temperature or heating rate coincides with the location of the estimated heat flux. The new method involves the solution to a Volterra equation of the second kind, which is inherently more stable than Volterra equations of the first kind. The solution for heat flux from a measured temperature is generally a first kind Volterra equation. Estimates from the new approach are compared to estimates from measured temperatures. The heating rate measurements are accomplished by leveraging the temperature dependent decay rate of thermographic phosphors (TGP). Results indicate that the new data-reduction method is far more stable than the usual minimization of temperature residuals, which results in errors that are 1.5–12 times larger than those of the new approach. Furthermore, noise in TGP measurements was found to give an uncertainty of 4% in the heating rate measurement, which is comparable to the noise introduced in the test case data. Results of the simulations and the level of noise in TGP measurements suggest that this novel approach to heat flux determination is viable. [DOI: 10.1115/1.1915389]

Introduction

Aerospace vehicles often encounter deleterious heating environments during high-speed flight. Accurate characterization of heating loads, then, is crucial to survivability of aerospace structures. In controlled tunnel tests, prediction of a heat flux incident on a test article can provide meaningful information concerning the environment that a full-scale structure will experience, whereas temperature measurements typically do not scale well from tunnel to flight conditions. Herein lies the necessity to predict heat fluxes. However, characterization of heating loads (or heat flux) in tests is not trivial because direct measurement is difficult.

Although the prediction of heat fluxes contains inherent challenges, several methods have evolved to accomplish the task with varying degrees of success. The most obvious approach to predicting heat fluxes is direct measurement with a heat flux gauge [1,2]. These gauges usually consist of a thermopile and actually measure temperature differences across a thin substrate. Assuming that the thermal conductivity and thickness of the substrate can be characterized, the heat flux can be calculated in terms of the temperature difference using Fourier's law. However, this approximation assumes that the temperature distribution in the sensor is linear, which, for transient conditions, is not strictly valid. The approximation theoretically improves as the thickness of the substrate is reduced. However, the signal to noise ratio is also reduced for thin substrates. Consequently, heating loads with high frequency transients cannot be measured accurately [1]. In general the problems associated with measurements from heat flux gauges include slow response time, flow disturbance, calibration and limited spatial resolution.

Alternatives include direct measurement via a calorimeter [3]. The heat flux can be obtained by measuring the temperature change in time of a known thermal mass. Like the heat flux gauge, these devices often suffer from slow response time and flow disturbance. Furthermore, the estimation of the heat flux from the actual measurement is complicated by the fact that the heat load may not be uniform across a surface because of lateral heat conduction [4]. Recently, new techniques for heat flux determination such as thermochromatic liquid crystals (TLC) [5] have become more popular. Conceptually, this process involves layers of crystals in thin films aligning themselves based on temperature gradients. The orientation can be inferred from spectral measurements of reflected light. The technique can provide high-density surface measurements but currently suffers from lagging response times [6] and a limited temperature range.

An attractive alternative for predicting heat fluxes is the direct measurement of temperature followed by a data reduction technique to estimate the incident flux [7] (often called the inverse heat conduction problem). In general, temperature measurement can be accomplished with acceptable precision and accuracy [8] with high frequency components [9] compared to heat flux measurements. In fact, thin film temperature measurements have become so robust and used so extensively to predict heat fluxes that the literature will often incorrectly refer to these types of measurements as heat flux measurements. However, this approach introduces its own set of difficulties. It is well known that the inverse heat conduction problem is ill-posed in the sense of Hadamard [10]. To be considered well-posed, solutions must have the following properties: existence, uniqueness, and stability. The inverse heat conduction problem is often formulated as an integral equation, which fails the uniqueness and stability tests [11]. This means that error in the heat flux estimate is unbounded [11, Theorem 1.17]. Consequently, random noise in the measurement, which is unavoidable, may become arbitrarily large.

When the conduction problem is linear and one-dimensional, analytic solutions can often be obtained for the heat flux using Duhamel's theorem [12,13]. These solutions often contain unacceptable errors [14] and lateral conduction effects are difficult to resolve [15]. Numerical analogs to these analytic methods have been developed to handle nonlinear conduction problems [16]. Unfortunately, these methods require numerical derivatives, which only exacerbate the instabilities of inverting the conduction equation [11,17].

To deal with the inherent instability of inverse problems, many researchers have developed techniques to damp large oscillations

Contributed by the Heat Transfer Division for publication in the JOURNAL OF HEAT TRANSFER. Manuscript received: August 19, 2003; final manuscript received: October 5, 2004; Review conducted by: George S. Dulikravich.

in the solution, such as regularization [18] and future time methods [7]. These approaches require a certain amount of bias to be added to the solution and they usually relax the exact matching of data to obtain a "fit" of the measured data by the model. The residual, which is the difference between the model temperature and the measurement, is minimized with respect to the unknown flux. Although these solution methods have proven to be extremely practical and successful, the solution requires a bit of art. Too much bias and the solution will not match the data; too little bias and the solution will contain large oscillations. Note that these solution approaches have been studied extensively, and the appropriate level of bias is usually obtained by requiring the residual to be of the order of the measurement noise [11].

Despite the apparent difficulties of reducing temperature data, the advantages of temperature measurement devices coupled with inverse techniques make this approach to heat flux determination attractive. For example, because temperature measurement devices are usually thinner than heat flux gauges [19], the time response is much better and the effect on the incident flows can be minimized. In addition, temperature measurements are easier to calibrate and the data reduction is not limited to one-dimensional estimation [20]. Therefore, it can be argued that temperature measurements and inverse data reduction techniques are preferable.

Despite advances in techniques devised to solve ill-posed problems and account for noisy data, the fact remains that appropriate data reduction remains a balancing act between introducing smoothing bias and amplification of noise. In many cases, solutions still contain unacceptable errors [12]. The present work suggests that many of the stability problems associated with the inverse heat conduction problem can be mitigated by measuring a different quantity, namely the heating rate [21,22]. The heating rate in the present context is defined as the time rate of change of temperature for a given location and time. It will be shown that the data reduction is inherently more stable if this quantity could be measured. However, no method existed (until now) to measure the heating rate directly. The heating rate approach represents a departure from typical heat flux determination methods such as those discussed briefly above, because the temperature is not explicitly required for the estimation of heat flux.

If the heating rate could be measured, the solution of the conduction equation for an unknown boundary flux becomes a Volterra equation of the second kind. It is well known that first kind Volterra equations are ill-posed in the sense of Hadamard [10], and that second-kind equations are not. In fact, many inverse solutions involve approximating the ill-posed equation by converting it to a Volterra equation of the second kind [23].

The objectives of the present work are to demonstrate a stable method for estimating heat flux from measured heating rates and to describe a technique to measure heating rate. The estimation component involves test problems with specific boundary/initial conditions and simulated noise, which is a common approach to evaluating inverse methods. The measurement technique involves the temperature sensitive decay rate of thermographic phosphors (TGP) [24]. Although TGPs have been used to measure temperature (particularly for remote measurement), the current approach will leverage particular properties of TGPs to obtain measurements, which are proportional to the heating rate, not temperature.

Thermographic phosphors are rare-earth-doped ceramics that fluoresce when exposed to ultraviolet radiation or similar excitation. In general, the intensity, frequency line shift, and decay rate are all temperature dependent. As a result, they have been used for remote temperature sensing in many applications [25]. Many materials have been used and tuned for specific applications with a great deal of success [26–28]. However, they have never been used to predict a heating rate. It is the strong dependence of the decay rate on temperature that will be leveraged to acquire a heating rate. This simple proof-of-concept described herein demonstrates the ability to extract heat fluxes with far greater accuracy than previously possible.

Theory

The following linear heat diffusion example will be used for illustration purposes. Assume one-dimensional conduction in a slab of length L. The governing equation for temperature change is given as

$$\frac{\partial^2\theta}{\partial\eta^2}=\frac{\partial\theta}{\partial\xi},\quad 0<\eta<1,\quad \xi>0, \tag{1}$$

subject to the boundary conditions

$$-\left.\frac{\partial\theta}{\partial\eta}\right|_{\eta=0}=Q(\xi), \tag{2}$$

$$\theta(1,\xi)=0, \tag{3}$$

and the initial condition

$$\theta(\eta,0)=0. \tag{4}$$

The spatial and temporal coordinate have been nondimensionalized (i.e., $\eta=x/L$, $\xi=\alpha t/L^2$, where α is the thermal diffusivity). The heat flux $Q(\xi)$ at $\eta=0$ is a continuous function of ξ and is presumed known. Using integral transforms, the infinite series solution is found to be [29]

$$\theta(\eta,\xi)=2\sum_{m=1}^{\infty}\cos(\beta_m\eta)\int_0^{\xi}Q(\xi')e^{\beta_m^2(\xi'-\xi)}d\xi', \tag{5}$$

where the eigenvalues are the positive roots of $\cos(\beta_m)=0$, i.e., $\beta_m=(2m-1)\pi/2$ where $m=1,2,3,\ldots$.

If the heat flux $Q(\xi)$ is unknown, Eq. (5) is a Volterra equation of the first kind for a known temperature, and the solution is unstable for discrete temperature measurements. Because TGP measurement is an optical technique, measurements can only be made on the surface ($\eta=0$). If we assume that the temperature on the surface is measured at N discrete times, then an estimate for the unknown heat flux can be found using standard inverse solution techniques. It can be argued that because measurements are restricted to the boundary, inverse methods are not required. In this case, the measured surface temperature can be treated as a boundary condition for the forward conduction solution. The heat flux can then be obtained by differentiating this solution. Because measurements are discrete and contain noise, however, inverse techniques can serve to stabilize the solution [14].

In the present work, the solution for the heat flux from measured temperatures involves inverting Eq. (5). For simplicity, we assume that the time increment between each discrete measurement is constant ($\Delta\xi$) and that the integral over all times in Eq. (5) is written as a summation of integrals over each time step. The discrete temperature solution at the surface then becomes

$$Y_r=2\sum_{m=1}^{\infty}\sum_{i=1}^{r}\int_{\xi_{i-1}}^{\xi_i}Q(\xi')e^{\beta_m^2(\xi'-\xi_r)}d\xi', \tag{6}$$

where Y indicates that the temperature is a discrete measurement at the surface, not a continuous function, and r indexes time such that $\xi_r=r\Delta\xi$, $r=0,1,2,\ldots$ and $Y(\xi_r)=Y_r$. Now, the heat flux is approximated analytically by assuming a piecewise integrable function $Q(\xi')$ over each time step and solving for the unknown function parameters at each time step. Note that a piecewise constant assumption would theoretically work here. However, the summation in the heating rate formulation (developed later) does not converge in a finite number of terms without additional assumptions. Therefore the following linear approximation is considered:

$$Q(\xi') = Q_i - \frac{Q_i - Q_{i-1}}{\Delta\xi}(\xi_i - \xi'), \tag{7}$$

where $\Delta\xi$ is the time step size, $\xi_{i-1} < \xi' \leqslant \xi_i$, and $Q_i = Q(\xi_i)$. The integration can be performed analytically leading to a set of N algebraic equations

$$Y_r = 2\sum_{m=1}^{\infty}\left\{\sum_{i=1}^{r}\frac{Q_i}{\beta_m^2}[e^{\beta_m^2(\xi_i-\xi_r)} - e^{\beta_m^2(\xi_{i-1}-\xi_r)}] - \sum_{i=1}^{r}\frac{Q_i - Q_{i-1}}{\beta_m^4\Delta\xi}[e^{\beta_m^2(\xi_i-\xi_r)} - e^{\beta_m^2(\xi_{i-1}-\xi_r)}(1+\beta_m^2\Delta\xi)]\right\}. \tag{8}$$

Note that Y_0 and Q_0 are assumed to be zero. The solution of the foregoing expression leads to an estimate of the heat flux at each time step.

The proposed approach to predicting heat flux requires measurement and calculation of the heating rate. A heating rate can be found analytically by differentiating Eq. (5) with respect to time. The formulation for heating rate, given as

$$\Lambda(\eta,\xi) = \frac{\partial\theta}{\partial\xi}(\eta,\xi) = 2\sum_{m=1}^{\infty}\cos(\beta_m\eta)\left[Q(\xi) - \beta_m^2\int_0^{\xi}Q(\xi')e^{\beta_m^2(\xi'-\xi)}d\xi'\right], \tag{9}$$

suggests that the nature of the solution for heat flux is not as ill-conditioned because Eq. (9) is a Volterra equation of the second kind [30,31]. The solution approach for heat flux follows the solution from a measured temperature by evaluating Eq. (9) at the surface ($\eta=0$) and inverting. As before, the heat flux can be calculated analytically by assuming an integrable form of the heat flux over the time step and integrating. It is not immediately clear that the infinite series in Eq. (9) converges in a finite number of terms because $\Sigma_{m=1}^{\infty}Q(\xi)\to\infty$. In fact, convergence cannot be guaranteed for all functions (see Appendix). However, the Appendix shows that the infinity cancels for reasonable choices of $Q(\xi')$. For this reason, the piecewise linear function for heat flux [Eq. (7)] was chosen. This approach represents one of the simplest functions that is integrable and whose series also converges.

As before, the heat flux is determined at each time when a heating rate is measured at the surface ($\eta=0$). The integral of Eq. (9) is converted to a sum of integrals over each time step giving

$$H_r = 2\sum_{m=1}^{\infty}\left[Q_r - \beta_m^2\sum_{i=1}^{r}\int_{\xi_{i-1}}^{\xi_i}Q(\xi')e^{\beta_m^2(\xi'-\xi_r)}d\xi'\right], \tag{10}$$

where r indexes the measurements and H indicates a discrete measurement, not a continuous function. Similarly, $H_r = H(\xi_r)$ and $Q_r = Q(\xi_r)$ is implied. After applying the piecewise linear heat flux [Eq. (7)], a set of N algebraic equations is recovered as

$$H_r = 2\sum_{m=1}^{\infty}\left\{Q_r - \sum_{i=1}^{r}Q_i[e^{\beta_m^2(\xi_i-\xi_r)} - e^{\beta_m^2(\xi_{i-1}-\xi_r)}] + \sum_{i=1}^{r}\frac{Q_i - Q_{i-1}}{\beta_m^2\Delta\xi}[e^{\beta_m^2(\xi_i-\xi_r)} - e^{\beta_m^2(\xi_{i-1}-\xi_r)}(1+\beta_m^2\Delta\xi)]\right\}. \tag{11}$$

See the Appendix for full development and convergence of Eq. (11). Now the unknown heat fluxes can be solved algebraically given the heating rate measurements.

The approach for estimating heat fluxes from both measured temperatures and measured heating rate is an exact matching technique often called Stolz's method [32]. While this is not strictly an inverse method because no bias is introduced to smooth the solution, the point of the present work is to demonstrate how the use of heating rate measurements does not require the introduction of bias to obtain stable solutions. Therefore, the exact matching approach will be used to highlight the difference between the methods.

The measurement of heating rate from TGPs is not a direct measurement. Instead, the intensity of phosphor emission is measured at a sample rate that is higher than the decay rate. After a phosphor is excited (usually by an ultraviolet light pulse), the concentration of excitation centers (excited electrons) is governed by the differential equation [33]

$$\tau\frac{dn}{dt} + n = 0, \tag{12}$$

where τ is the lifetime of an excitation center. Assuming that τ is a constant in time, the solution can be written as

$$\frac{I}{I_o} = \frac{n}{n_o} = \exp\left[-\frac{t}{\tau}\right], \tag{13}$$

where the intensity I is proportional to n, and I_o and n_o are values at the beginning of the decay. The decay time τ can be estimated from a series of intensity measurements collected during the decay. If we assume that the phosphor has been completely and carefully characterized, the decay time is a material property that is a well-known function of temperature. Calibration curves are generated that relate τ to temperature for a given phosphor. By estimating τ from a single pulse, we can deduce the temperature from these calibration curves. This approach is commonly used to predict temperature from phosphor decay measurements [33]. For many interesting engineering problems, though, the temperature is not constant in time. Because the lifetime τ is generally a function of temperature, we expect τ to change in time as well. Therefore, we have augmented the model in Eq. (13) to use a first-order Taylor series expansion of the decay time to introduce the derivative of τ. Now the normalized intensity,

$$\frac{I}{I_o} = \exp\left[-\frac{t}{\tau + \frac{d\tau}{dt}t}\right], \tag{14}$$

contains three parameters (I_o, τ, and $d\tau/dt$) that are estimated from a series of intensity measurements using standard parameter estimation techniques [34]. This simplistic approach is strictly valid for small variations in temperature only because the derivative of the decay time is considered to be a perturbation of τ. In general, $\tau(T(t))$, so if the temperature changes significantly, the governing equation for electron concentration, must be solved for specific time dependencies of τ on time. For steady-state data (as in the present analysis), $d\tau/dt$ should be identically zero. Therefore, this approximation is justified for the present work.

The heating rate can now be computed using the chain rule as

$$\frac{d\theta}{dt} = \frac{d\theta}{d\tau}\frac{d\tau}{dt}, \tag{15}$$

where $d\theta/d\tau$ is a temperature dependent material property and is derived from the same calibration curves used to obtain temperature from decay time. The parameter of interest ($d\tau/dt$) is obtained through a fit of intensity measurements. Through test cases, we will demonstrate that prediction of $d\tau/dt$ and subsequent data reduction of $d\theta/dt$ to heat flux is inherently more stable than estimating heat flux from temperature measurements.

Results

Data reduction. To compare different methods for predicting heat flux, a known analytic function was chosen as the exact heat flux, Q, to which all estimates will be compared. Table 1 lists each type of heat flux that was examined. The exact analytic solutions to both the temperature, Y, and the heating rate, H, [Eqs. (5) and

Table 1 Reported values are norms of the error between the exact heat flux, Q, and the estimated heat flux Q_e, i.e., $|Q-Q_e|$ where e corresponds to the type of estimate given by the column labels

Test Case	Y	Y_n	H	H_n	H_d
zero	0	1.5171	0	0.1178	0.9488
triangle	0.0006	1.5171	0.0006	0.1181	0.9656
sine	0.3998	1.5509	0.9215	0.9149	1.9987
square	0.4914	1.4693	0.9735	0.9363	1.1972

(9), respectively] were calculated to provide the measurement data from which the estimates were derived. The time step is $\Delta\xi=0.02$ giving 51 samples within the $\xi=1$ duration of the experiment. Normally distributed random noise was added to the measurements to evaluate how the estimators behave when measurement error exists in the temperature, Y_n, and heating rate, H_n. The magnitude of the noise added to the temperature data has a standard deviation of $\sigma=0.02$, which provides visual evidence of errors in the temperature for unity heat fluxes.

To provide a meaningful and fair comparison between the heating rate and temperature estimation approaches, it is not clear how much noise should be added to the heating rate data. After all, the noise is primarily a function of the measurement equipment, which is entirely different than temperature measurement devices. As a first approximation, the same noise level could be added to both data sets. However, for a given heat flux, the magnitude of the variation in heating rate is larger than the variation in temperature. For example, given a triangular heat flux with a value of unity at the peak, the maximum temperature rise is approximately 0.5. The maximum heating rate is approximately 2. Therefore, the signal is 4 times that of the temperature data. Consequently, to make the signal to noise ratio between the two data sets comparable, a noise level of 0.08 was added to the heating rate data to obtain H_n. Of course the relative magnitude of each signal varies depending on the heat flux. Nevertheless, the triangular heat flux was considered to be representative of all fluxes tested and in all cases the amount of noise added to the heating rate was four times that added to the temperature data. Note that this approach hardly seems fair in the zero flux case, when there should be zero signal.

To provide an additional comparison, a second heating rate is generated by differencing the noisy temperature data Y_n. Because noisy data is being differentiated, we expect errors associated with these data H_d to be large. Table 1 reports the error norms $|Q-Q_e|$, where Q is the exact heat flux and Q_e is the estimated heat flux indicated in the table for each set of fabricated data. In general, the errors associated with estimation based on the heating rate are less than the errors for the temperature data.

The estimates were obtained assuming a piecewise linear heat flux as described in Eqs. (11) and (8). In the case of zero flux and triangular flux, the linear approximation matches exactly with the analytic heat flux. Therefore, the error in the estimates using exact data (Y and H in Table 1) are nonzero but small. These values are nonzero because the infinite series is approximated with a finite number of terms. The number of terms used in each case was 2000. The norm of the error associated with 2000 terms is of the order of 10^{-4} for the triangular case. Using exact data for the sine case, for example, still yields a nonzero error because the integral of the piecewise linear approximation does not match the analytic solution exactly.

To establish the statistical significance of the difference between the estimates derived from different data, the sample mean $\bar{x}$ and sample variance s^2 of the errors for each simulation were calculated. Further, the distributions were checked for normality by plotting the standardized normal scores against the observed errors. A linear shape verified that all errors are normally distributed. To ensure that none of the methods contain significant bias

Table 2 Significance test for variance of errors between the temperature case and the indicated heating rate approach. For values greater than $F(0.05;50,50)=1.6125$, the hypothesis that the variances are equal must be rejected.

Test Case	H_n	H_d
zero	166.2	2.560
triangle	166.2	2.471
sine	2.898	0.602
square	2.472	1.507

in the solution—meaning that the estimates were consistently either over- or underpredicted—the calculated mean of the error was compared to a mean of zero. In all cases, the significance test, given by

$$\frac{\bar{x}-\mu_0}{s/\sqrt{n}} \geqslant t(\alpha;n-1), \quad \mu_0=0, \tag{16}$$

was satisfied for the two-sided 95% confidence level. Therefore, the use of Eqs. (8) and (11) do not introduce significant bias. Evaluation of the "quality" of the estimates proceeds from a comparison of the variances. Because the focus of this work is to evaluate the heating rate approach to that of a temperature measurement approach, the null hypothesis assumes that variances of the errors between any two estimates are equal. If the null hypothesis is accepted, the two approaches generate estimates whose errors are statistically similar. The alternative hypothesis is that the variance of the temperature approach (σ_1^2) is larger than that of any other approach (σ_2^2).

$$H_0:\sigma_1^2=\sigma_2^2 \tag{17}$$

$$H_1:\sigma_1^2>\sigma_2^2 \tag{18}$$

Because we are claiming that noise becomes amplified, the variance of the noise is a good measure of the amount of amplification. The ratio of variances has an F-distribution $[F(\alpha;N,N)=s_1^2/s_2^2]$ for given degrees of freedom $N=n-1=50$ for both samples [35]. At a confidence level of 95%, $F=1.6125$. Therefore, the null hypothesis must be rejected for any ratio greater than 1.6125, which means that the difference in the variance is statistically significant. Table 2 shows the values for the comparison between errors from the temperature approach and the two heating rate approaches. Based on this significance test, the only simulations where the variance could not be considered significantly different is Q_{H_d} for the sinusoidal and square heat flux cases. In all other tests, the null hypothesis is rejected and the heating rate approach is considered "better" than the temperature approach.

The first test case examined is the zero heat flux. The exact surface temperature is zero in this case, but the temperature signal with added noise is nonzero and shown in Fig. 1. From the zero heat flux, a zero heat rate is also found (shown in Fig. 2 along with noisy data). The first noisy signal H_n was obtained by adding normally distributed random values with a standard deviation of $\sigma=0.08$ (four times the noise assigned to the temperature signal) to the zero signal. The second noisy signal was generated by calculating a backward difference of the noisy temperature data Y_n. This is a simplistic approach to obtaining a heating rate that demonstrates how noise in the temperature is amplified by differencing. The standard deviation of noise inherent to H_d is $s=0.95$, which is nearly 50 times that of the temperature data and more than 11 times that of H_n.

Heat flux estimates for the zero flux case are shown in Fig. 3 for the noisy temperature and heating rate data sets. It is immediately

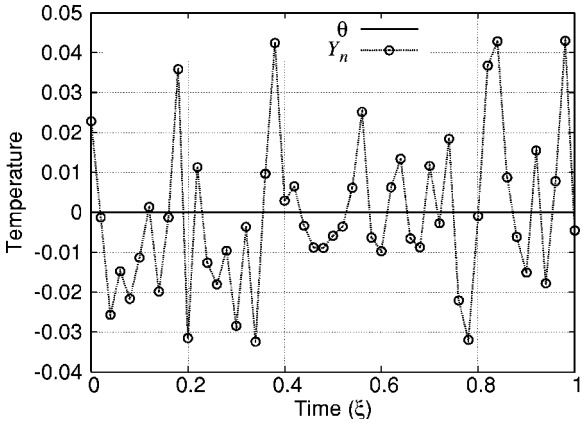

Fig. 1 The temperature response to a zero heat flux is shown with and without added noise. The normally distributed random noise has a standard deviation of $\sigma=0.02$. Lines are added to guide the eye.

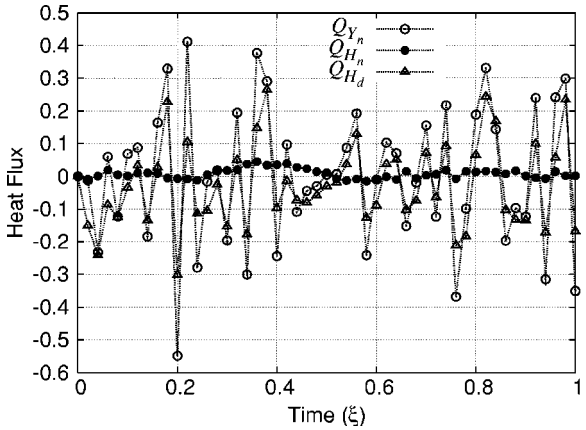

Fig. 3 The heat flux estimates of the zero flux case from temperature measurements Y_n, heat rate measurements H_n and differenced temperatures H_d. The lines connecting the estimates merely guide the eye.

obvious that the estimates produced from the heating rate data are far superior to estimates from temperature data. As listed in Table 1, the norm of the errors is 12.9 times larger for the temperature data and 8.05 times larger for the differenced heating rate data as compared to the noisy heating rate data H_n. Ironically, the differencing of temperature data H_d seems to produce better estimates than the temperature data Y_n. This plot and the reported errors also indicate how much the errors are amplified. Table 3 shows the error in the estimate normalized by the error in the measurement. This ratio of error in the estimate to error in the measurement (noise) is given as

$$E/N = \frac{|Q - Q_{Y_n}|}{|Y - Y_n|}, \tag{19}$$

where the temperature data and estimates can be replaced by the corresponding heating rate data and estimates. For the estimates from temperature measurements Y_n, the error to noise ratio is approximately 11 for the triangular and zero flux cases, but the error to noise ratio of estimates from the heating rate H_n is 0.2 and from differenced heating rate H_d is 0.1. The E/N ratio for H_d is so low because the noise level in the signal is so high. Therefore, this metric does not allow quantitative evaluation of the estimates from measurements but provides a sense of how each method amplifies the noise. In fact, the E/N ratio for both H_d and H_n should be comparable when compared to the E/N ratio for Y_n.

The next test case examined is the triangular heat flux, whose surface temperature history is shown in Fig. 4 with and without additional noise. As in the zero flux case, the noisy signal is obtained by adding a normally distributed random component with standard deviation of $\sigma=0.02$. Visually, the noise is a small percentage of the actual signal ($\sim 4\%$). The noisy temperature history is used to predict heat fluxes by inverting Eq. (5) with the method described above. This is inherently an unstable process, and the estimate from noisy data, Q_{Y_n} in Fig. 5 shows that small errors become amplified in the solution. No attempt to relax the

Table 3 Amplification of noise can be deduced from the ratio of the norm of the errors in the estimate to the norm of the noise in the measurements. Larger numbers indicate that the amplification of noise is greater.

Test Case	Y_n	H_n	H_d
zero	11.14	0.293	0.106
triangle	11.14	0.194	0.106
sine	11.39	1.506	0.100
square	10.79	1.541	0.111

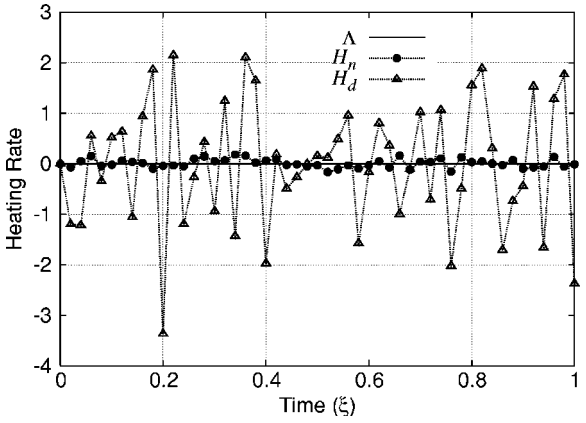

Fig. 2 The heating rate response to a zero heat flux is shown with and without added noise. The normally distributed random noise (H_n) has a standard deviation of 0.08, and a central differencing of the noisy temperature Y_n is used to produce H_d, which has a standard deviation of 0.94. The lines connecting the points merely guide the eye.

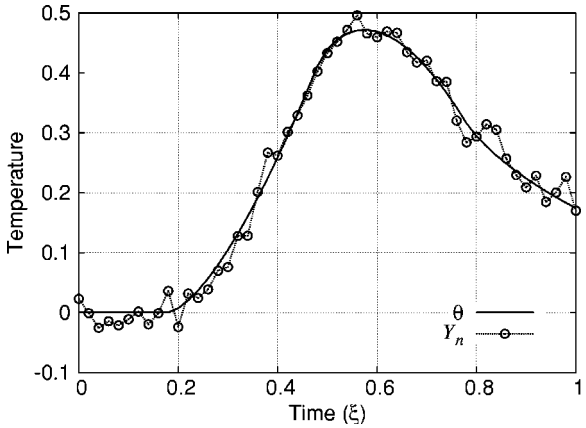

Fig. 4 The exact temperature response to a triangular heat flux profile (see Fig. 5). The noisy signal has a normally distributed random noise with standard deviation $\sigma=0.02$.

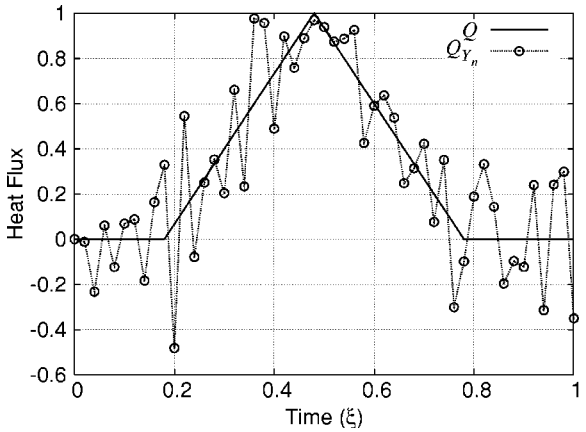

Fig. 5 The heat flux history estimates are derived from the temperatures in Fig. 4. The estimate from noisy data, Q_{Y_n}, demonstrate how small errors become amplified. The lines merely guide the eye.

solution, introduce bias or otherwise implement any stabilization technique was made. In practice, a true inverse procedure would be implemented to achieve less noisy results than the exact matching procedure used here. In fact, the zero residual method (often called Stolz's method [32]) is a worst-case scenario. However, the method was chosen to illustrate that estimates from a noisy heating rate can provide reasonable and accurate estimates without bias. Figure 6 shows the estimates produced from the heating rate data sets, which are shown in Fig. 7. Both sets of estimates appear to match the exact solution closer than the estimates in Fig. 5. Note how closely the heating rate measurements with noise H_n visually matches the exact solution. The results suggest that direct matching solution of the Volterra equation of the second kind is not nearly as sensitive to measurement errors as the Volterra equation of the first kind. In fact, the error in the noisy estimate, Q_{H_n} appears to be damped, and the solution contains little bias and almost no noise. However, the surprising feature is that Q_{H_d}, which was produced from a signal H_d (open triangles in Fig. 7) whose noise is 20% of the actual signal, faithfully reproduces the original heat flux with errors comparable to Q_{Y_n}. Table 1 demonstrates that the estimates from all varieties of the heating rate (H, H_n, and H_d) contain very little error.

The next case examined (sine-wave heat flux) does not have an analytic solution that can be modeled exactly with a piecewise

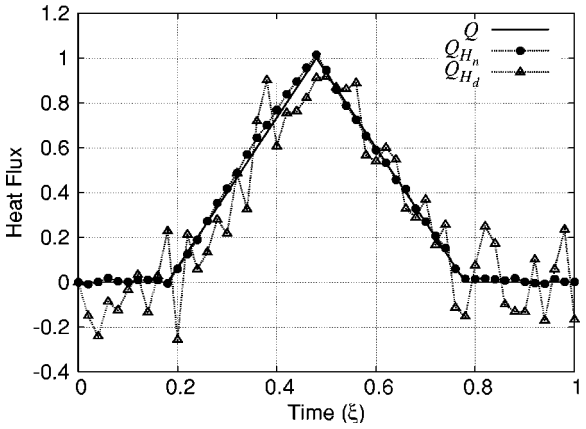

Fig. 6 Heat flux estimates derived from heating rate data using an exact matching scheme. Noise in the measured data is not amplified as in case of temperature data. The lines merely guide the eye.

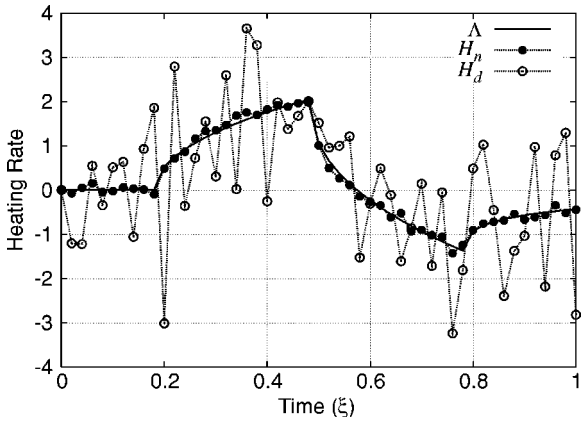

Fig. 7 Heating rate measurement data for the triangular case with an without added noise are shown. The lines merely guide the eye.

linear approximation. Therefore, there is an error inherent to the estimates even with exact data. For this demonstration, a sinusoidal heat flux with a frequency of the order of the Nyquist frequency was selected. The high-frequency component in this data will further exercise the methods. The exact temperature response to a sine-wave heat flux is shown in Fig. 8. Similarly the heating rate measurements are shown in Fig. 9. In both cases, even the exact data appear to be noisy because of the piecewise linear approximation and the high-frequency content of the heat

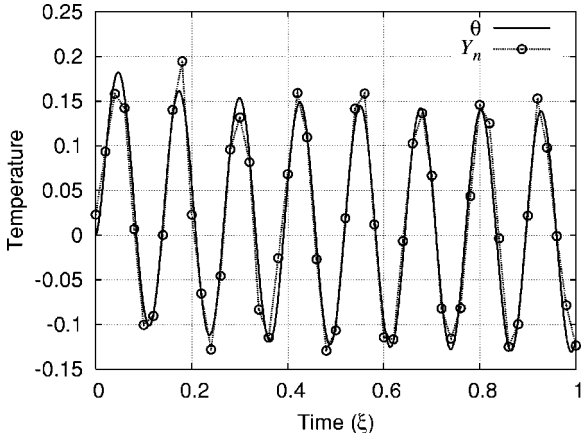

Fig. 8 Temperature solution to a sin wave heat flux with and without added noise

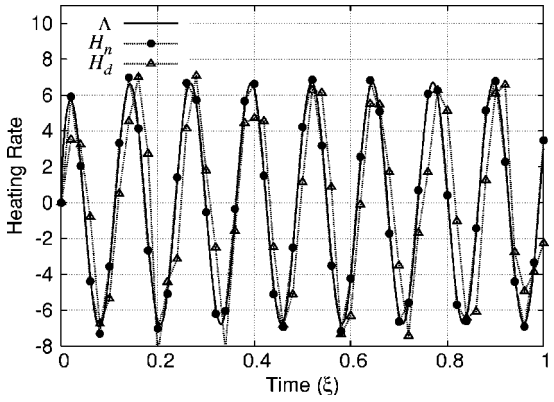

Fig. 9 Heating rate measurements of the sinusoidal heat flux with and without noise

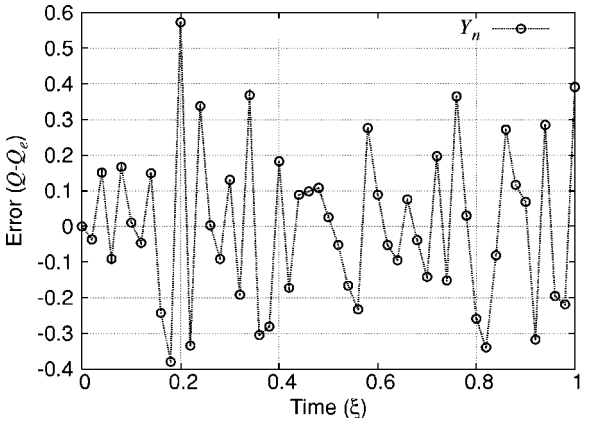

Fig. 10 Error in the heat flux estimates derived from temperature measurements for the sinusoidal case

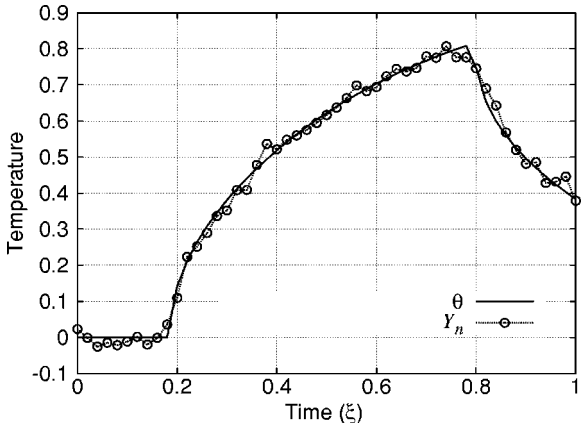

Fig. 12 Temperature solution to a square wave heat flux with and without added noise

flux.

Figures 10 and 11 show the difference in the flux instead of the actual estimate (i.e., $Q-Q_e$). The apparent periodicity of the error in the estimates from the heating rate measurements (Fig. 11) indicate some bias in the solution. In fact, the heating rate under predicts the flux by an average of 12% at the peaks. The bias is a result of the piecewise linear approximation and, incidentally, is still smaller than the error associated with the estimates derived from temperature data (see Fig. 10).

The final test case is particularly interesting because of the discontinuity inherent to a square flux. At the point when the flux is instantaneously turned on, the heating rate would theoretically be infinite. A measurement of this sort is not physically possible, and a piecewise linear approximation of the flux will not capture this discontinuity. However, the temperature remains finite and measurable. Therefore, we expect significant errors at the times when the flux is turned on and off for the hating rate case and errors similar to previous test cases for the temperature measurements. Temperature measurements and heating rate measurements are shown in Figs. 12 and 13, respectively. Note that the magnitude of the heating rate is large at the discontinuity compared to the other test cases. Also, the reader is reminded that the amount of noise added to the measurements is 0.02 and 0.08 to the temperature and heating rate measurements respectively. The estimates derived from temperature measurements (Fig. 14) exhibit the usual amplification of noise as the previous test cases. However, the estimates derived from heating rates (Fig. 15) show somewhat different behavior than the previous test cases. The heating rate measurement does not capture the discontinuity well. In fact, the error shows up as a bias for all times after the jump. Interestingly, the norm of the error is comparable to that from temperature measurements. Nevertheless, noise is often more desirable than bias if an experimenter must choose between the two. This artifact, however, does not necessarily mean that heating rate can not be considered a desirable quantity to measure. For example, Fig. 16 shows how

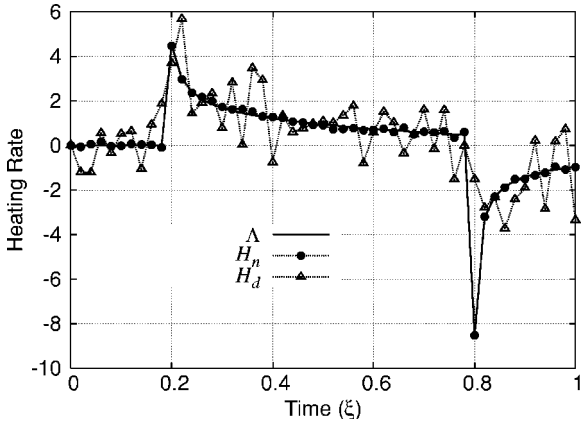

Fig. 13 Heating rate measurements of the square heat flux with and without noise

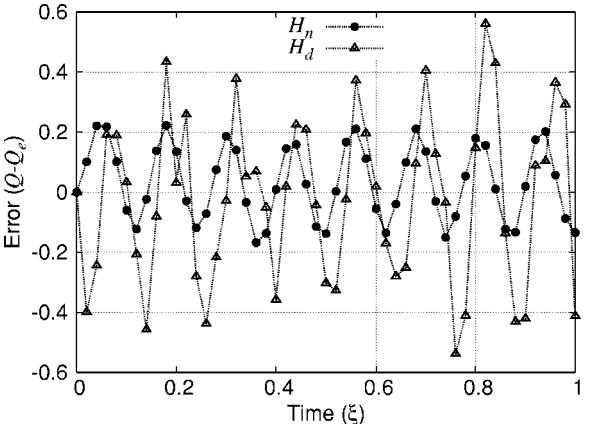

Fig. 11 Error in the heat flux estimates derived from heating rate data for the sinusoidal case

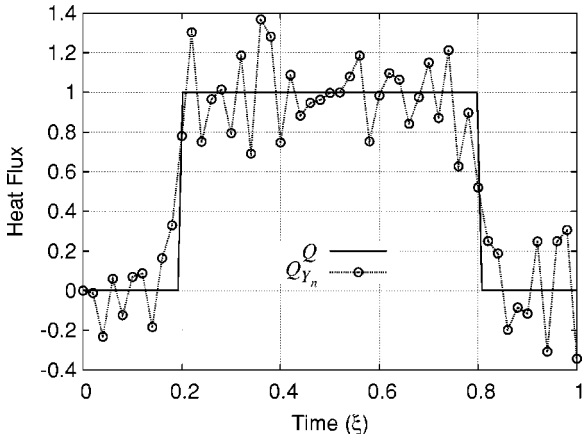

Fig. 14 The heat flux history estimates are derived from the temperatures in Fig. 12. The estimate from noisy data, Q_{Y_n}, demonstrate how small errors become amplified. The lines merely guide the eye.

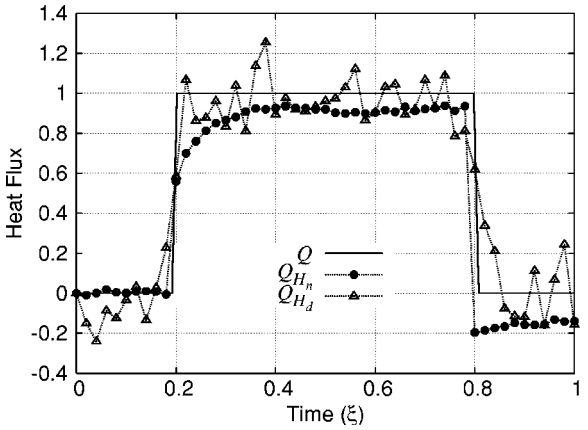

Fig. 15 Heat flux estimates derived from heating rate data (see Fig. 13) using an exact matching scheme. Noise in the measured data is not amplified as in case of temperature data. The lines merely guide the eye.

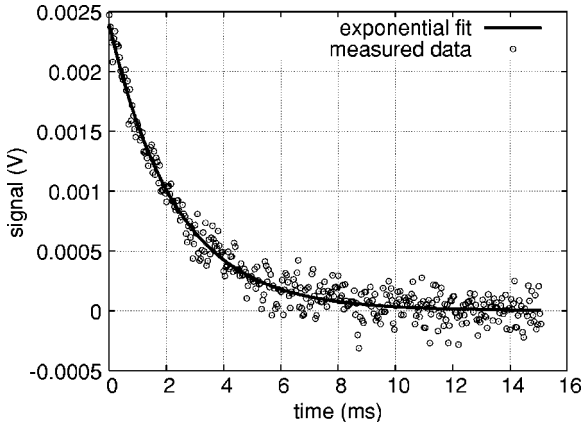

Fig. 17 Phosphor emission from $La_2O_2S:Eu$ after LED excitation was turned off. The data was translated so that the peak emission occurs at $t=0$ ms. Fitting parameters are shown in Table 4.

the error (and therefore, bias) decreases with increased sample rate, which is contrary to temperature measurement behavior. In fact, for high sample rates, errors associated with temperature data are orders of magnitude greater than those associated with heating rate measurements. Consequently, the possibility for eliminating bias in the heating rate estimates exists, but measurement noise is omnipresent in estimates from temperature data.

Estimation of τ by decay measurement. As a demonstration of heating rate determination, the phosphor $La_2O_2S:Eu$ was measured at steady state to characterize the effects of noise. Single shot data are shown in Fig. 17 along with an exponential fit of the data [see Eq. (13)]. The estimated parameters are $\tau=2.31$ ms and $I_0=0.00239$ V. At steady state, the heating rate, and therefore the change in decay time, is expected to be near zero. Therefore estimates of the decay time τ should be consistent between models [Eqs. (13) and (14)] and the change in the decay time $d\tau/dt$ from Eq. (14) should be negligible. From the estimates using the new model [Eq. (14)], the decay time is 2.21 ms, which is 5% different than the constant model, and the change in decay time is 0.022 s/s, which is smaller than the noise in the estimate for τ and considered negligible. Because of the noise in the measured signal, the change in heating rate is nonzero. However, note that photomultiplier tube (PMT) measurements are inherently noisy and no electronic means were used to smooth or average the data. Despite the noise, the change in decay time has little contribution to the overall intensity decay (see Table 4). Further the decay times predicted from each model are consistent. As a side effect of the estimation procedure, we can also obtain the maximum intensity, which is also consistent between models. The errors in the estimates given by 95% confidence intervals is of the order of the noise introduced in the data reduction test cases discussed in the previous section. Therefore, the magnitude of the errors observed in the estimates of the test cases is comparable to what we might expect to obtain from TGP measurements.

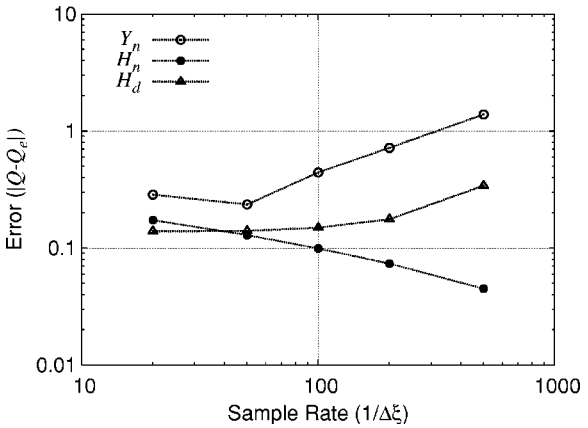

Fig. 16 Norm of the error for estimates derived from the measurements indicated on a log–log scale. Errors are normalized with the total number of samples.

Based on noise in the steady-state single-shot measurement, we can evaluate the errors in the estimation procedure when the temperature changes during the decay. Data were fabricated by assuming $\tau=2.31$ ms from the actual measurement. Then an artificial $d\tau/dt=0.3$ was added in Eq. (14) to obtain a new intensity measurement. The error due to noise in the actual measurement was then superimposed onto the exact signal, resulting in noisy data that includes a nontrivial change in decay time. Figure 18 shows the fit of fabricated data using the typical constant decay model [Eq. (13)] and the new model, which includes the change in the decay time [Eq. (14)]. If the decay time changes, as in the foregoing example, then a significant difference between the fits of Eqs. (13) and (14) are seen (Fig. 18). Table 5 gives the estimated parameters for the foregoing example. Agreement between the linearly varying model and the fabricated data is exceptional demonstrating that the measurement noise may not affect heating rate determination from phosphor measurements. However, transient measurements need to be made to verify the utility of the method.

The uncertainty in the $d\tau/dt$ estimate is 3.3% of the actual estimate. In addition, the uncertainty in the estimate of τ is 4.2% of the actual estimate. Because the estimate of τ and estimate of $d\tau/dt$ are related to temperature and heating rate, respectively, the data suggest that noise in each measurement should also be ~4%. In fact, this is the level of noise that was used in the preceding example test cases. Therefore, these measurements from TGPs indicate that the example test cases are valid estimates of the errors we expect to see in practice.

Conclusions

A new approach to predicting heat flux is proposed, which may improve heat flux estimates by reducing instabilities inherent in temperature to heat flux data reduction methods. By measuring the heating rate, the integral equation for heat flux becomes a Volterra equation of the second kind, which is inherently more stable than the first kind. Analysis confirms that the method is more stable and can accommodate more noise than an approach that uses tem-

Table 4 Estimates of decay time parameters based on measured phosphor data

	I_o (V)	τ (ms)	$d\tau/dt$
constant	$2.33 \times 10^{-3} \pm 2.76 \times 10^{-5}$	2.31 ± 0.038	n/a
linear	$2.42 \times 10^{-3} \pm 3.3 \times 10^{-5}$	2.21 ± 0.080	0.022 ± 0.0153

Table 5 Estimates of decay time parameters based on fabricated phosphor data

	I_o (V)	τ (ms)	$d\tau/dt$
exact	2.33×10^{-3}	2.31	0.3
constant	$1.93 \times 10^{-3} \pm 2.93 \times 10^{-5}$	5.20 ± 0.116	n/a
linear	$2.40 \times 10^{-3} \pm 3.6 \times 10^{-5}$	2.27 ± 0.095	0.303 ± 0.010

perature measurements. The method for measuring heating rate uses thermographic phosphors, which is already being used to measure temperatures.

Evaluations of the measurement technique indicate that the TGP measurement noise is similar in magnitude to temperature measurement noise. Consequently, estimates from heating rate data are expected to be much more stable and accurate than estimates from temperature measurements. Therefore, TGPs may prove to be an excellent heat flux determination technique where surface measurements can be made optically.

However, the example measurements are preliminary and future work will improve the reliability of the estimates. Furthermore, work needs to be done to characterize TGPs for these types of measurements. For example, the decay rate, excitation frequency, emission frequency, temperature range, and proximity sensitivities need to be tuned for each application. Despite the work that needs to be performed to raise the process to a production level, significant and inherent advantages can be seen from the foregoing proof-of-concept.

Acknowledgments

The author would like to thank Steve Allison at Oak Ridge National Laboratory for his experience and knowledge on making thermographic phosphor measurements and to Jay Frankel at the University of Tennessee for useful conversations on reduction of heat rate data. Furthermore, encouragement and guidance was provided by John Ahner in the Mathematics Department at Vanderbilt. The author would like to thank the reviewers whose comments and persistence greatly strengthened the paper.

Nomenclature

t = time
H = heating rate measurements or hypothesis
I = phosphor emission intensity
L = conduction domain length
Q = normalized heat flux
M = number of terms in the series
N = number of measurements
R = residual
Y = measured temperatures

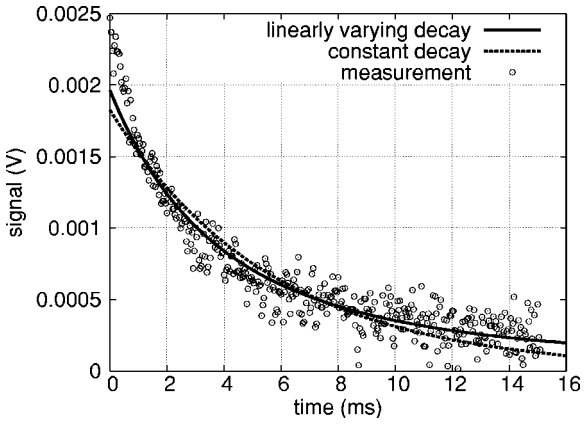

Fig. 18 Fit of fabricated noisy emission data using the constant and linear decay models

Greek

β = eigenvalues
θ = normalized temperature change
η = normalized spatial dimension
Λ = normalized heating rate
τ = phosphor decay time
ξ = normalized time
Φ = basis functions

subscripts/superscripts

d = difference
i = summation index
m = eigenvalue index
n = noisy
o = initial value
r = measurement index

Appendix

It is not immediately clear that the heating rate Eq. (9), evaluated at the surface will converge because of the first term in the summation.

$$\Lambda(\xi) = 2\sum_{m=1}^{\infty}\left[Q(\xi) - \beta_m^2\int_0^{\xi} Q(\xi')e^{\beta_m^2(\xi'-\xi)}d\xi'\right]. \tag{20}$$

Using integration by parts, the integral term can be expressed as

$$\beta_m^2\int_0^{\xi} Q(\xi')e^{\beta_m^2(\xi'-\xi)}d\xi' = [Q(\xi')e^{\beta_m^2(\xi'-\xi)}]_0^{\xi} - \int_0^{\xi}\frac{dQ(\xi')}{d\xi'}e^{\beta_m^2(\xi'-\xi)}d\xi' \tag{21}$$

$$= Q(\xi) - Q(0)e^{-\beta_m^2\xi} - \int_0^{\xi}\frac{dQ(\xi')}{d\xi}e^{\beta_m^2(\xi'-\xi)}d\xi' \tag{22}$$

Now the heat flux $Q(\xi)$ in Eq. (22) cancels with the heat flux in Eq. (20) to give an equivalent infinite series

$$\Lambda(\xi) = 2\sum_{m=1}^{\infty}\left[Q(0)e^{-\beta_m^2\xi} + \int_0^{\xi}\frac{dQ(\xi')}{d\xi'}e^{\beta_m^2(\xi'-\xi)}d\xi'\right] \tag{23}$$

Now the offending infinity has been eliminated. Because $0 < \xi' < \xi$, each term in the series contains an exponential with a negative exponent. As the eigenvalue increases, all terms will approach zero if the heat flux derivative is a bounded function. This assumption is not unreasonable because it represents a physical quantity and will not likely approach infinity. However, the series still may not converge because the value of the exponential will approach unity at the upper limit of the integral. Therefore, the convergence is undetermined because the function is pointwise bounded, not uniformly bounded.

Despite our inability to prove convergence in general, we can show that certain discretized forms of Eq. (20) do converge. Note that Eq. (23) should not be discretized directly as in Eq. (10), unless the first term is also summed and evaluated at the beginning of each discrete time step.

If we assume that the heat flux can be approximated by some piecewise function, the integral in Eq. (20) can be expressed as a sum of integrals

$$H_r = 2\sum_{m=1}^{\infty}\left\{ Q_r - \beta_m^2 \sum_{i=1}^{r} \int_{\xi_{i-1}}^{\xi_i} Q(\xi') e^{\beta_m^2(\xi'-\xi_r)} d\xi' \right\}, \quad (24)$$

where the functions are evaluated at discrete times, such that $\xi_r = r\Delta\xi$, $r=1,2,3,\ldots$, $\xi_0=0$, $H_r=H(\xi_r)$, $H_0=0$, $Q_r=Q(\xi_r)$, $Q_0=0$.

Now assume that the heat flux is given by some integrable function between time steps. The simplest is perhaps a constant, such that the value during the time step is also the value at the later time step.

$$Q(\xi') = Q_i, \quad \xi_{i-1} < \xi' \leqslant \xi_i. \quad (25)$$

Because $Q(\xi)$ is a constant, it can be taken outside of the integral, and the integral can be evaluated exactly.

$$H_r = 2\sum_{m=1}^{\infty}\left\{ Q_r - \beta_m^2 \sum_{i=1}^{r} Q_i \frac{1}{\beta_m^2}\left[e^{\beta_m^2(\xi_i-\xi_r)} - e^{\beta_m^2(\xi_{i-1}-\xi_r)}\right] \right\}. \quad (26)$$

The final term in the internal summation can be evaluated separately to obtain

$$H_r = 2\sum_{m=1}^{\infty}\left\{ Q_r - Q_r\left[1 - e^{-\beta_m^2\Delta\xi}\right] - \sum_{i=1}^{r-1} Q_i\left[e^{\beta_m^2(\xi_i-\xi_r)} - e^{\beta_m^2(\xi_{i-1}-\xi_r)}\right] \right\}. \quad (27)$$

The advantage of this is that now the offending infinity in the outer summation has been canceled.

$$H_r = 2\sum_{m=1}^{\infty}\left\{ Q_r e^{-\beta_m^2\Delta\xi} - \sum_{i=1}^{r-1} Q_i\left[e^{\beta_m^2(\xi_i-\xi_r)} - e^{\beta_m^2(\xi_{i-1}-\xi_r)}\right] \right\}. \quad (28)$$

Each term in the summations can be expressed as some constant (the heat flux at a point in time the sum of exponential). All the exponential terms can be expressed with an integer multiple of $\Delta\xi$ as

$$e^{-\beta_m^2 n\Delta\xi}, \quad n = 1,2,3,\ldots. \quad (29)$$

By examining the ratio of subsequent terms in each infinite sum,

$$\lim_{m\to\infty}\frac{a_{m+1}}{a_m} = \lim_{m\to\infty}\frac{e^{[(2m+1)\pi/2]^2 n\Delta\xi}}{e^{[(2m-1)\pi/2]^2 n\Delta\xi}} = r, \quad (30)$$

we can determine whether the summation will converge. Following Cauchy, if the value of the limit r is less than one, the infinite summations will converge by the ratio test [36]. In the present case, the limit approaches zero,

$$r = \lim_{m\to\infty} e^{-2m\pi^2 n\Delta\xi} = 0, \quad (31)$$

for any positive n and m. Because each summation will converge, the entire the equation converges.

Note that convergence can only be found as an artifact of the discretization. For example, if we define the constant heat flux to be the value at the time preceding the step,

$$Q(\xi') = Q_{i-1}, \quad \xi_{i-1} \leqslant \xi' < \xi_i, \quad (32)$$

the convergence is not so well behaved. In this case, the discrete heat rate is given as

$$H_r = 2\sum_{m=1}^{\infty}\left\{ Q_r - \beta_m^2 \sum_{i=1}^{r} Q_{i-1} \frac{1}{\beta_m^2}\left[e^{\beta_m^2(\xi_i-\xi_r)} - e^{\beta_m^2(\xi_{i-1}-\xi_r)}\right] \right\}, \quad (33)$$

once the constant heat flux is removed from the integral and the integral is evaluated. Similar to the previous example, we can evaluate the final term of the summation separately.

$$H_r = 2\sum_{m=1}^{\infty}\left\{ Q_r - Q_{i-1}\left[1 - e^{-\beta_m^2\Delta\xi}\right] - \sum_{i=1}^{r-1} Q_{i-1}\left[e^{\beta_m^2(\xi_i-\xi_r)} - e^{\beta_m^2(\xi_{i-1}-\xi_r)}\right] \right\}. \quad (34)$$

In this case, we end up with a term where $n=0$. The limit given by Eq. (31) approaches one and convergence is undetermined.

For a piecewise linear heat flux approximation as presented in Eq. (7), the heating rate is given by Eq. (11). By considering the term where $i=r$ separately as before, Eq. (11) becomes

$$H_r = 2\sum_{m=1}^{\infty}\left\{ Q_r - Q_r\left[1 - e^{-\beta_m^2\Delta\xi}\right] - \sum_{i=1}^{r-1} Q_i\left[e^{\beta_m^2(\xi_i-\xi_r)} - e^{\beta_m^2(\xi_{i-1}-\xi_r)}\right] + \frac{Q_r - Q_{r-1}}{\beta_m^2\Delta\xi}\left[1 - e^{-\beta_m^2\Delta\xi}(\beta_m^2\Delta\xi - 1)\right] + \sum_{i=1}^{r-1}\frac{Q_i - Q_{i-1}}{\beta_m^2\Delta\xi}\left[e^{\beta_m^2(\xi_i-\xi_r)} - e^{\beta_m^2\Delta\xi}(\beta_m^2\Delta\xi - 1)\right] \right\}. \quad (35)$$

The Q_r terms cancel. All other terms except one contain an exponential with a negative exponent, which has already been shown to converge [see Eq. (31)]. The last term to consider is

$$\frac{Q_r - Q_{r-1}}{\Delta\xi}\sum_{m=1}^{\infty}\frac{1}{\beta_m^2} = \frac{Q_r - Q_{r-1}}{\Delta\xi}\frac{4}{\pi^2}\sum_{m=1}^{\infty}\frac{1}{(2m-1)^2}. \quad (36)$$

It can be shown that $\Sigma_{m=1}^{\infty} 1/m^p$ converges if and only if $p>1$ (Corollary 4.3.7 from Belding and Mitchell [36]). Because $1/m^2 > 1/(2m-1)^2$ for large m, the series in Eq. (36) converges by the comparison test. Now because each series in the equation converges, the equation for heating rate converges.

References

[1] Holmberg, D. G., and Diller, T. E., 1995, "High-frequency heat flux sensor calibration and modeling," J. Fluids Eng., **117**, pp. 659–664.

[2] Piccini, E., Guo, S. M., and Jones, T. V., 2000, "The development of a new direct-heat-flux gauge for heat-transfer facilities," Meas. Sci. Technol., **11**, pp. 342–349.

[3] Diller, T. E., and Kidd, C. T., 1997, "Evaluation of numerical methods for determining heat flux with a null point calorimeter," in *Proceedings of the 42nd International Instrumentation Symposium*, Research Triangle Park, NC, pp. 251–262.

[4] Buttsworth, D. R., and Jones, T. V., 1997, "Radial conduction effects in transient heat transfer experiments," Aeronaut. J., **101**, pp. 209–212.

[5] Ireland, P. T., and Jones, T. V., 2000, "Liquid crystal measurements of heat transfer and surface shear stress," Meas. Sci. Technol., **11**, pp. 969–986.

[6] Newton, P. J., Yan, Y., Stevens, N. E., Evatt, S. T., Lock, G. D., and Owen, J. M., 2003, "Transient heat transfer measurements using thermochromic liquid crystal. Part 1: An improved technique," Int. J. Heat Fluid Flow, **24**, pp. 14–22.

[7] Beck, J. V., Blackwell, B., and St. Claire, Jr., C. R., 1985, *Inverse Heat Conduction: Ill-Posed Problems*, Wiley–Interscience, NY.

[8] Guo, S. M., Lai, C. C., Jones, T. V., Oldfield, M. L. G., Lock, G. D., and Rawlinson, A. J., 1998, "The application of thin-film technology to measure turbine-vane heat transfer and effectiveness in a film-cooled, engine-simulated environment," Int. J. Heat Fluid Flow, **19**, pp. 594–600.

[9] Dinu, C., Beasley, D. E., and Figliola, R. S., 1998, "Frequency response characteristics of an active heat flux gage," J. Heat Transfer, **120**, pp. 577–582.

[10] Hadamard, J., 1923, *Lectures on Cauchys Problems in Linear Partial Differential Equations*, Yale University Press, New Haven, CT.

[11] Kirsch, A., 1996, *An Introduction to the Mathematical Theory of Inverse Problems*, Springer, Berlin, Vol. 120.

[12] Cook, W. J., 1970, "Determination of heat transfer rates from transient surface temperature measurements," AIAA J., **8**, pp. 1366–1368.

[13] Kendall, D. N., and Dixon, W. P., 1966, "Heat transfer measurements in a hot shot wind tunnel," IEEE Trans. Aerosp. Electron. Syst., **AES-3**, pp. 596–603.

[14] Walker, D. G., and Scott, E. P., 1997, "Evaluation of estimation methods for high unsteady heat fluxes from surface measurements," AIAA J., **12**, pp. 543–551.

[15] Buttsworth, D. R., and Jones, T. V., 1998, "A fast-response high spatial resolution total temperature probe using a pulsed heating technique," J. Turbomach., **120**, pp. 612–617.

[16] Dunn, M. G., George, W. K., Rae, W. J., Woodward, S. H., Moller, J. C., and

Seymour, P. J., 1986, "Heat flux measurements for the rotor of a full-stage turbine: Part II: Description of analysis technique and typical time-resolved measurements," ASME J. Turbomach., **108**, pp. 98–107.
[17] Ehrich, F. F., 1954, "Differentiation of experimental data using least squares fitting," J. Aeronaut. Sci., **22**, pp. 133–134.
[18] Tikhonov, A. N., and Arsenin, V. Y., 1977, *Solutions of Ill-Posed Problems*, V. H. Winston & Sons, Washington, D.C.
[19] George, W. K., Rae, W. J., Seymour, P. J., and Sonnenmeier, J. R., 1987, "An evaluation of analog and numerical techniques for unsteady and heat transfer measurements with thin film gauges in transient facilities," in *Proceedings of the ASME/JSME Thermal Engineering Joint Conference*, Honolulu, HI, Vol. 2, pp. 611–617.
[20] Walker, D. G., Scott, E. P., and Nowak, R. J., 2000, "Estimation methods for 2D conduction effects of shock-shock heat fluxes from temperature measurements," AIAA J., **14**, pp. 533–539.
[21] Frankel, J. I., and Keyhani, M., 1999, "Inverse heat conduction: The need for heat rate data for design and diagnostic purposes," in *Proceedings of the 18th LASTED International Conference on Modeling, Identification and Control*, Innsbruck, Austria, February.
[22] Frankel, J., and Osborne, G., 2004, "Motivation for the development of heating/cooling rate and heat flux rate sensors for engineering applications," in *Proceedings of the 42nd AIAA Aerospace Sciences Meeting and Exhibit.*
[23] Lamm, P. K., 1995, "Future-sequential regularization methods for ill-posed volterra equations," J. Math. Anal. Appl., **195**, pp. 469–494.
[24] Walker, D. G., and Schetz, J. A., 2003, "A new technique for heat flux determination," in *Proceedings of the ASME Summer Heat Transfer Conference*, Las Vegas, NV.
[25] Allison, S. W., and Gillies, G. T., 1997, "Remote thermometry with thermographic phosphors: Instrumentation and applications," Rev. Sci. Instrum., **68**, pp. 2615–2650.
[26] Sholes, R. R., 1980, "Fluorescent decay thermometry with biological applications," Rev. Sci. Instrum., **51**, pp. 882–884.
[27] Feist, J. P., and Heyes, A. L., 2000, "The characterization of $Y_2O_2S:Sm$ powder as a thermographic phosphor for high temperature applications," Meas. Sci. Technol., **11**, pp. 942–947.
[28] Allison, S. W., Cates, M. R., Noel, B. W., and Gillies, G. T., 1988, "Monitoring permanent-magnet motor heating with phosphor thermometry," IEEE Trans. Instrum. Meas., **37**, pp. 637–641.
[29] Necati Özişik, M., 1968, *Boundary Problems of Heat Conduction*, Dover, New York.
[30] Kress, R., 1989, *Linear Integral Equations*, Vol. 82 in Applied Mathematical Sciences, Springer-Verlag, Berlin.
[31] Corduneanu, C., 1991, *Integral Equations and Applications*, Cambridge University Press, Cambridge.
[32] Stolz, Jr. G., 1960, "Numerical solutions to an inverse problem of heat conduction for simple shapes," J. Heat Transfer, **82**, pp. 20–26.
[33] Shionoya, S., and Yen, W. M., editors, 1999, *Phosphor Handbook*, CRC Press, Boca Raton.
[34] Beck, J. V., and Arnold, K. J., 1977, *Parameter Estimation in Engineering and Science*, Wiley, New York.
[35] Hogg, Robert V., and Ledolter, Johannes, 1992, *Applied Statistics for Engineers and Physical Scientists*, 2nd ed., Macmillan, NY.
[36] Belding, D. F., and Mitchell, K. J., 1991, *Foundation of Analysis*, Prentice–Hall, NJ.